

# Self-assembling antimicrobial peptides on nanotubular titanium surfaces coated with calcium phosphate for local therapy

Hilal Yazici<sup>a</sup>, Gizem Habib<sup>a</sup>, Kyle Boone<sup>b</sup>, Mustafa Urgan<sup>c</sup>, Feride Sermin Utku<sup>a,d</sup>, Candan Tamerler<sup>b,e,\*</sup>

<sup>a</sup> Department of Molecular Biology and Genetics, MOBGAM, Molecular Biology, Biotechnology and Genetic Center, Istanbul Technical University, 34469 Maslak, Istanbul, Turkey

<sup>b</sup> Bioengineering Program, Institute for Bioengineering Research, University of Kansas, Lawrence, KS 66045, USA

<sup>c</sup> Department of Material Science and Engineering, Istanbul Technical University, 34469 Maslak, Istanbul, Turkey

<sup>d</sup> Department of Biomedical Engineering, Yeditepe University, 34755 Istanbul, Turkey

<sup>e</sup> Department of Mechanical Engineering, University of Kansas, Lawrence, KS 66045, USA

## ARTICLE INFO

### Keywords:

Implant infections  
Hydroxyapatite-binding peptide  
Calcium-phosphate coatings  
Nanotubular titanium  
Self-assembled peptides  
Antimicrobial peptides

## ABSTRACT

Bacterial infection is a serious medical problem leading to implant failure. The current antibiotic based therapies rise concerns due to bacterial resistance. The family of antimicrobial peptides (AMP) is one of the promising candidates as local therapy agents due to their broad-spectrum activity. Despite AMPs receive increasing attention to treat infection, their effective delivery to the implantation site has been limited. Here, we developed an engineered dual functional peptide which delivers AMP as a biomolecular therapeutic agent onto calcium phosphate (Ca-P) deposited nanotubular titanium surfaces. Dual functionality of the peptide was achieved by combining a hydroxyapatite binding peptide-1 (HABP1) with an AMP using a flexible linker. HABP functionality of the peptide provided a self-coating property onto the nano-topographies that are designed to improve osteointegration capability, while AMP offered an antimicrobial protection onto the implant surface. We successfully deposited calcium phosphate minerals on nanotubular titanium oxide surface using pulse electrochemical deposition (PECD) and characterized the minerals by XRD, FT-IR, FE-SEM. Antimicrobial activity of the engineered peptide was tested against *S. mutans* (gram-positive) and *E. coli* (gram-negative) both in solution and on the Ca-P coated nanotubular titanium surface. In solution activity of AMP and dual functional peptide have the same Minimum Inhibitory Concentration (MIC) (32 mg/mL). The peptide also resulted in the reduction of the number of bacteria both for *E. coli* and *S. mutans* compare to control groups on the surface. Antimicrobial features of dual functional peptides are strongly correlated with their structures suggesting tunability in design through linkers regions. The dual-function peptide offers single-step solution for implant surface functionalization that could be applicable to any implant surface having different topographies.

## 1. Introduction

Titanium and titanium alloys are widely used materials for dental and orthopedic implants due to their superior properties [1,2]. Nonetheless, they still face improper implant–tissue integration with the surrounding bone that often occurs due to unwanted biological responses, starting with bacterial colonization, then bacterial infection and, finally, fibrous capsule formation. The success of implants depends not only on the bone-implant integration, but also the prevention of bacterial infection [3,4]. Thus, bacterial infection and osteointegration are still major challenges in implantation. In all cases, biological

response is related with the surface properties of implants; therefore, surface modifications are essential to enhance the biocompatibility, osteoconductivity, and antimicrobial properties of biomaterials [4,5].

To prevent bacterial infection, several surface modification strategies have been applied, besides conventional systematic antibiotic treatment, such as development of non-fouling surfaces, functionalization of surfaces with antibiotics, and biocidal substances. The effectiveness of each strategy depends on various parameters such as type of pathogen in case of creating non-fouling surfaces, spectrum of activity for the chosen antibiotic drug as well development of antibiotic resistance in a relatively short time period, and systemic toxicity for

\* Corresponding author at: Institute for Bioengineering Research, Department of Mechanical Engineering, Bioengineering Program, University of Kansas, 1530 W, 15th St, Learned Hall, Lawrence, KS 66047, USA.

E-mail address: [ctamerler@ku.edu](mailto:ctamerler@ku.edu) (C. Tamerler).

<https://doi.org/10.1016/j.msec.2018.09.030>

Received 16 November 2017; Received in revised form 17 August 2018; Accepted 10 September 2018

Available online 12 September 2018

0928-4931/ © 2018 Elsevier B.V. All rights reserved.

biocides because of high doses [4,6,7]. Therefore, alternative strategies need to be developed.

There is a clear need for a broad-spectrum antimicrobial substance that prevents bacterial colonization on implant surfaces, minimizes bacterial resistance with displaying long-term stability and has a low cytotoxicity profile. Antimicrobial peptides have the potential to meet these criteria due to their superior microbiocidal characteristics and broad spectrum compared to synthetic and semi-synthetic antibiotics [6,8–10]. AMPs are less likely to cause pathogen resistance and are thus very appealing. Although AMPs are promising candidate for the new generation of antimicrobial surfaces [11,12], applications of AMPs are limited with their systemic well distribution. The problem in distribution of AMPs sometimes requires the use of high concentration of peptides that may bring toxicity problems. Their rapid protease digestion and peptide aggregation are also another challenge to utilize them as systematic antimicrobial agents. They are good candidates for local therapy to prevent bacterial infection at the implant site compare to convectional antibiotics [4,7,13]. AMPs would be an intriguing alternative to classical antibiotics without causing side effects and with their low toxicity profile [14]. Thus, stable immobilization of AMPs on implant surfaces could be the way to overcome all limitations with increasing their long-term stability and activity [10,11,12,15–18].

Various covalent immobilization strategies that are based on chemical-coupling reactions have been applied for AMP immobilization on various materials such as metals including titanium [19–22] polymeric brushes and resins [23–25] and glass cover slips [26]. Among them, self-assembled monolayers (SAMs) of thiol- and silane-based molecules are widely used for biological surface modification of implant materials. However, they suffer as suitable functional molecular candidates applied onto nano- to micro-porous Ca-P coatings due to their limitation to apply over the surfaces with different topographies and stiffness as well as their surface chemistries. Their application requires the presence of functional groups, which are non-specific to surfaces and synthetic pathways, and it necessitates complex chemistry. They have also limited control on the orientation of the antimicrobial agent, which may restrict the agent's ability to retain biological activity. Their applicability is also limited to a range of implantable materials specifically metal and metal oxides (i.e., titanium-based materials, gold, platinum and glass) [27].

Ceramics and minerals are also one of the preferable materials in implantation. For example, the surface treatments of Ca-P based materials are also commonly used in dental and orthopedic applications due to their osteoconductive properties, and high loading capacity for antibiotics and antimicrobial agents [28–31]. Antibiotics however cannot be incorporated into the calcium phosphate coatings during its formation because of the extremely high processing temperature applied in plasma spraying. Moreover, physical absorption of the antimicrobial agents onto the surface of calcium phosphates limits the loaded amount and release characteristics [28,32,33]. There is therefore a need to find new ways to functionalize Ca-P surfaces with functional groups to create antimicrobial surfaces.

Next generation molecular linkers in creating antimicrobial surfaces are expected to induce controlled and predictable interactions at biomaterial interfaces with high material binding affinity and selectivity. These two properties can only be achieved with material surface recognition capability, which is necessarily specific to a desired surface. Having these properties may enable precise control of the density, the functionality and the accessibility of biomolecules [34,35]. During the last decade, material binding peptides possessing affinity and specificity to variety of inorganic surfaces have been generated using phage and cell surface display techniques [36,37]. Their potential use was increasingly demonstrated in various scientific disciplines including surface functionalization [36,38–40], biomineralization [41–43], tissue engineering [44] and regenerative medicine [45]. Application of surface-binding peptides to hard-tissue regeneration and restorative medicine is particularly intriguing and, consequently, there has been a great

deal of interest in identifying and characterizing peptides that bind to various biocompatible materials, such as TiO<sub>2</sub>, Au, SiO<sub>2</sub>, hydroxyapatite (HA), and selected polymers [38–40,44,46].

In the present study, an engineered chimeric peptide was designed as a self-assembled antimicrobial bio agent against *Escherichia coli* (*E. coli*) and *Streptococcus mutans* (*S. mutans*) to apply over the micro-porous Ca-P minerals coated onto nano-tubular titanium. The chimeric peptide is engineered to combine both antimicrobial and hydroxyapatite-binding peptide domains to achieve bioenabled self-assembly of the peptide in a single step. HABP1 was previously discovered in our group using a combinatorial biology based phage-display protocol [41]. This short peptide was synthesized in conjugation with an idealized AMP sequence through a triple glycine bridge. AMP motif, i.e. tet127 (KRWWKWWRR), was chosen from a study performed by Hilpert et al. [47] due to its high activity against *Pseudomonas aeruginosa* while covalently tethered on a substrate. This property makes the peptide very attractive to exhibit potent antimicrobial activity both in solution [48] as well as tethered form [47]. The efficiency of HABP1-AMP dual-functional was evaluated against *E. coli* and *S. mutans* in solution with a microdilution assay. Bacterial infection was next evaluated on the functionalized Ca-P coated nanotubular titanium surface with confocal microscopy (CM).

The proposed method eliminates complex surface functionalization procedures or the covalent modification of the implant surfaces that are coated with osteoconductive minerals. In a single step, bio-self assembly provides to combine the delivery of antimicrobial peptide over Ca-P coatings deposited on metallic implants having any nano- to micro-scale features. The approach is general and applicable to various biomaterials and implants surfaces, and may be a candidate for the prevention of implant infections for diverse kinds of medical devices.

## 2. Experimental section

### 2.1. Nanotubular titanium surface preparation and characterization

Sizes of 250 by 250 by 1 mm plates of commercially available pure titanium (cp grade) were incrementally ground utilizing #120 grit down to #1200 grit emery paper and wet polished in a one micrometer diamond paste, washed with distilled water and sonicated in acetone. The nanotubular titanium oxide surfaces were prepared in an electrochemical cell using a stainless steel cathode with an anodic constant voltage of 40 V in 0.5 wt% NH<sub>4</sub>F ethylene glycol solution at room temperature for 30 min. The total number of specimen was six. The crystalline structure and morphology of nanotubular surfaces were characterized using an X-ray diffractometer (Philips PW 3710) and a field emission scanning electron microscopy (SEM, XL-30-FEG, FEI, The Netherlands; and JEOL JSM 7000F FEI, The Netherlands), respectively.

### 2.2. Calcium phosphate coating and characterization

Nanotubular titanium surfaces were bioactivated by immersion in 0.5 M NaOH for 2 min at 50 °C and rinsed with deionized water to prevent crack-formation. A modified simulated body fluid, containing reagent grade 0.15 M NaCl, 1.67 mM K<sub>2</sub>HPO<sub>4</sub> and 2.50 mM CaCl<sub>2</sub>, pH buffered at 7.2 with the addition of 0.05 M Tris(hydroxyl amino-methane) (pH 7.4) and hydrochloric acid, was used as the supporting electrolyte solution. All chemicals were reagent grade. Deposition was conducted in a typical three-electrode electrochemical cell. The working electrode was the titanium sample, the reference electrode was a standard silver-silver chloride reference electrode (Ag/AgCl in saturated KCl) and the counter electrode was platinum. Deposition was carried out at 80 °C by pulsing the current density between  $-10 \text{ mA/cm}^2$  for 0.2 s and  $10 \mu\text{A/cm}^2$  for 10 s for 100 cycles and then maintaining at a constant cathodic current density of  $-10 \text{ mA/cm}^2$  for 60 min. Coated samples were characterized using an X-ray diffractometer (Philips PW 3710) and a FT-IR Spectrometer (Mattson

1000). FE-SEM cross-sectional images of CaP coated samples were obtained by forming a groove on the back of coated substrates, freeze-drying in liquid nitrogen for 30 s and then mechanically breaking the substrate to expose the length of nanotubes [49].

### 2.3. Peptide synthesis

Three different peptides (cHABP1, AMP, cHABP1-AMP) were synthesized by standard solid phase peptide synthesis technique on Wang resin (Novabiochem, San Diego, CA) using F-moc chemistry CSBio 336s (CSBio Inc., Menlo Park, CA) automated peptide synthesizer and HBTU activation was used for the synthesis. The resulting resin-bound peptides were cleaved and side-chain-deprotected using Reagent K (TFA/thioanisole/H<sub>2</sub>O/phenol/ethanedithiol (87.5:5:5:2.5)) and precipitated by cold ether. Obtained crude peptides were purified by RP-HPLC up to a > 98% purity (Gemini 10u C18 110A column). The purified peptides were checked by mass spectroscopy (MS) using a MALDI-TOF mass spectrometer.

### 2.4. Bacterial maintenance and culturing

Two different bacteria type, one gram-positive (*Streptococcus mutans*, ATCC® 25175™) and one gram-negative (*Escherichia coli*, ATCC® 25922™) were selected for measurement of antibacterial activity of newly designed dual-functional peptide. *E. coli* and *S. mutans* were cultured in LB (Luria Bertani) media and Brain Heart Infusion (Fluka, 53283) respectively and incubated at 37 °C with constant agitation (200 rpm) to proceed all experiments.

### 2.5. Broth Microdilution Antibacterial Assay for free peptides

The inhibition effect of the peptides in the presence of different concentrations was determined according to Broth Microdilution Antibacterial Assay of peptides. Briefly, serial dilutions of the each peptide (from 1, 2, 4 µg/mL to 256 µg/mL) were prepared in double distilled water (ddH<sub>2</sub>O) in 96-well microliter plates. Two different bacteria inoculum (*E. coli* and *S. mutans*), which were diluted from overnight culture, were allowed to grow exponential phase then incubated with the peptides to determine Minimum Inhibitory Concentration (MIC). A volume of 180 µL of test organism in proper media as described in previous section and 20 µL of peptide solutions at final concentrations of (from 1, 2, 4 µg/L to 256 µg/mL) were placed into 96-well plates and incubated at 37 °C for 16 to 20 h. Subsequently, growth inhibition was detected with spectrophotometric methods via optical density measurement at 600 nm. All experiments were repeated three times in duplicate for each bacterial strain.

### 2.6. Peptide surface modification

Prior to surface modification experiments, a mild cleaning procedure was employed to the HA-coated titanium surfaces. All surfaces were washed with DI water several times followed by mild vortexing. Washed surfaces were then sterilized under UV light for 10 min. The surfaces were then incubated overnight with PC buffer (55 mM KH<sub>2</sub>PO<sub>4</sub>, 45 mM Na<sub>2</sub>CO<sub>3</sub>, 200 mM NaCl) containing 0.1% detergent (combination of 20% (w/v) tween 20 and 20% (w/v) tween 80) for surface equilibration. To accomplish peptide-surface modification, surfaces were placed first in fresh buffer and then peptide solution was added to a 256 µg/mL final concentration in 1 mL total volume. Finally, surfaces were incubated overnight at room temperature with constant rotating (80 rpm) to allow peptide-surface interaction.

### 2.7. Anti-adhesive effect of peptides

Bacterial adhesion characteristics of functionalized HA-coated titanium surface were evaluated against one gram-positive (*S. mutans*) and

one gram-negative (*E. coli*) bacteria via cell spreading method. Briefly, both bacteria strains were cultured overnight in a proper media and conditions (as described above in bacterial strains section). A concentration of 10<sup>6</sup> cells/mL from the overnight culture was inoculated into fresh media and incubated until mid-log growth phase. The cultures were then centrifuged at 2700 rpm for 10 min and the supernatants were discarded. The precipitated cells were first washed twice with PBS, and then resuspended in 1.0 mL PBS at a concentration of 10<sup>7</sup> cells/mL. Then, the bacterial suspension was exposed onto each peptide-modified surface in a 24 well plate and incubated for 24 h at 37 °C. The surfaces were removed from the wells with sterile forceps and gently washed with PBS. Subsequently, surfaces were placed in broth and the attached bacteria were dislodged by mild ultrasonication for 2 min in an ultrasonic bath followed by rapid vortexing (10 s). Cell spreading method following serial ten-fold dilutions was used to determine the number of bacteria on the surface.

### 2.8. Bactericidal effect

The bacterial suspension (*E. coli* and *S. mutans*) as concentrated by centrifugation and resuspended in PBS at a concentration of 5 × 10<sup>7</sup> cfu/mL; 1 mL of the bacteria suspension was added to each substrate in 24-well plate. Slide chambers were covered and placed in a humidified incubator at 37 °C; after 2 h, nonadherent bacteria were removed with PBS. Adherent bacteria were stained with FITC (6 µg/mL) in PBS for 15 min at 37 °C. Slides were rinsed with PBS and visualized under confocal microscope (Leica TCS SP2 SE). Fluorescent (488-nm band-pass filter for excitation of FITC) images were taken at identical locations to determine stained with FITC.

### 2.9. Peptide structure generation

Structures of the peptides were generated with PyRosetta software using Robetta server library fragments and energy minimization routing. New structures were generated through five hundred decoys for each peptide. The secondary structure features recorded for each generated structure were the lengths of the alpha helices, the lengths of turns and the lengths of bends. DSSP was used to calculate the secondary structure features based on the three-dimensional atomic positions for each generated structure [50]. Rules were induced by the Modified Learning from Experience Module version 2 (MLEM2) [50,51]. The induced rules represent the secondary structure features that are specific to a single sequence among the three sequences (AMP, cHABP1, cHABP1-AMP) considered.

## 3. Results

### 3.1. Titanium surface preparations and characterization

FE-SEM image (Fig. 1) confirmed that the electrochemically treated pure titanium possessed orderly arrangements of nanotubular structures, with an average diameter of 90 nm and an average length of 2.5–3.0 µm [48,51,52]. The left inset is cross sectional view of the nanotubes and the right inset represents cross section of calcium phosphate deposition on nanotubular titanium.

### 3.2. Calcium phosphate coating on titanium surface and its characterization

FE-SEM of 2.4–3.2 µm thick CaP deposit on nanotubular titania confirmed the formation of a layer with uniformly distributed acicular crystals, approximately 150 nm in diameter, and 0.5 µm long, with Ca/P atomic ratios of 1.67–2.0 as shown in Fig. 2. The XRD spectrum (Fig. 2a) displayed the highest intensity peaks at 31.8°, 32.1°, and at 25° values of 2θ, typically observed in carbonated HA [49,52,53]. The FTIR spectrum (Fig. 3b), displayed phosphate peaks at 520–660, 961, and at 976–1190 cm<sup>-1</sup>; peak for –OH bend at 635 cm<sup>-1</sup>; peak for –OH



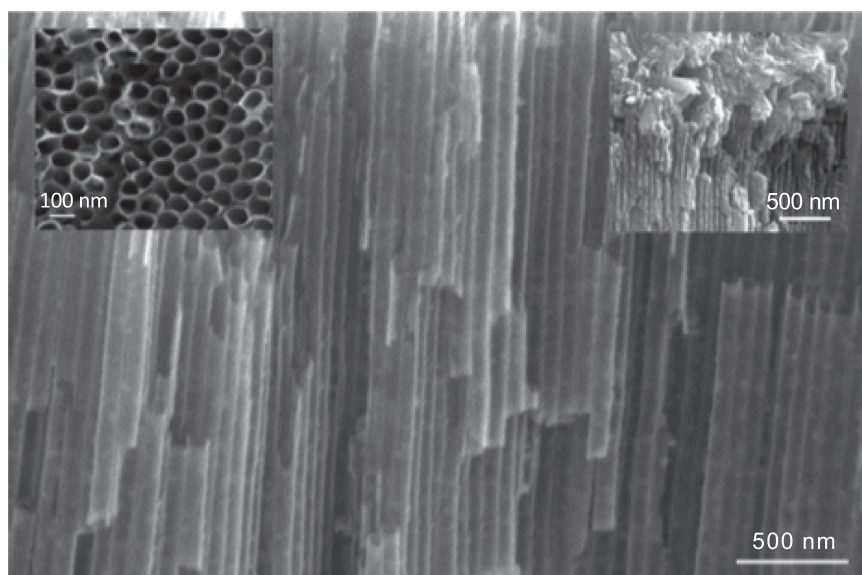


Fig. 1. FE-SEM image of nanotubular titania (A) and (B) at different magnification.

stretch at  $3650\text{ cm}^{-1}$ , which confirms the presence of hydroxyl in the structure; and carbonate peaks at  $875$  and  $1300\text{--}1650\text{ cm}^{-1}$ . The hydroxyl peaks in carbonated HA were less prominent than those observed in HA [52]. The compound was thus characterized to be a bi-phasic HA ( $\text{HA}$ ,  $\text{Ca}_{10}(\text{PO}_4)_6(\text{OH})_2$ ) and carbonated HA ( $\text{CHA}$ ,  $\text{Ca}_{10}(\text{PO}_4)_3(\text{CO}_3)_3(\text{OH})_2$ ).

### 3.3. Physiochemical properties of dual-functional peptides

Engineered dual-function peptide (cHABPI-AMP) has both material binding affinity to HA and high antimicrobial activity exhibiting simultaneously. Physicochemical characteristic and sequence information of peptides including the molecular weight (MW), isoelectric point (pI), charge and gravity values, which were calculated using the ExPASy Prot-Param tool of the Swiss Institute of Bioinformatics are listed in Table 1. The cHABPI demonstrated a low molecular weight (968.17) with no charge at pH 6.90 [41]. HHC36/Tet 127, which is

chosen from the literature, is a cationic peptide (charge of +5) with highest pI (12.31) compared to the other chosen peptides (Table 1), and has a wide antimicrobial spectrum [14,54,55]. The peptide, i.e. cHABPI-AMP, is designed to have a flexible –GGG–linker to provide enough flexibility for the peptide to ensure dual functionality. The dual-functional peptide demonstrated a cationic property (charge of +5), similar to the chosen AMP, but has lower pI value (10.93) compared to the AMP peptide (Table 1). The values of the hydropathy index of the each peptide were listed in Table 1 as GRAVY column. AMP has highly negative hydropathy index ( $-2.767$ ), with high potential for disturbing the cell membranes. On the contrary, cHABPI has positive hydropathy index ( $0.456$ ) with partially inhibiting bacterial reproduction. cHABPI-AMP has also negative hydropathy index ( $-1.048$ ) with both functionalities. Variations in hydropathy index suggest their complementary functions, although it is still difficult to make strong correlation in between hydropathy index and antimicrobial activity of peptides.

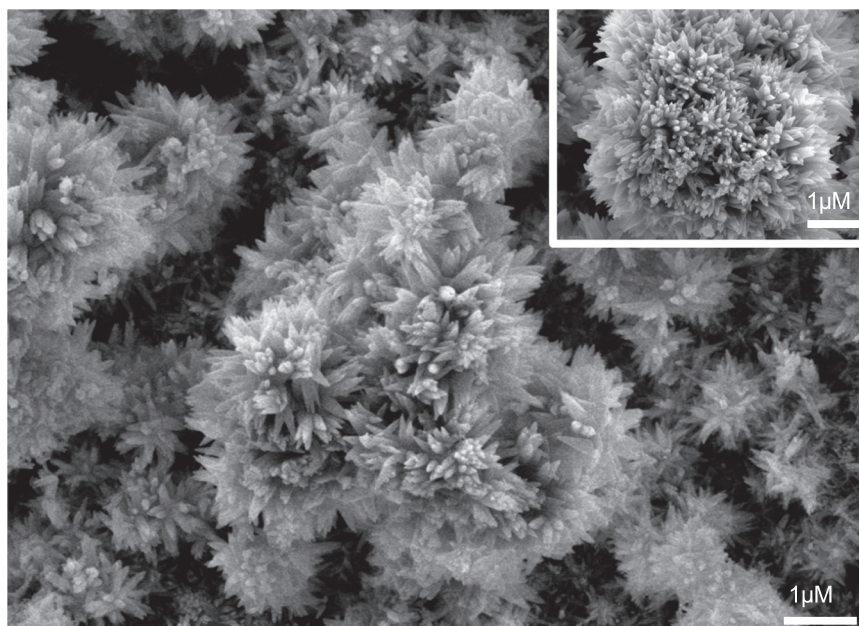


Fig. 2. FE-SEM image of HA deposition on nanotubular titania at different magnification.

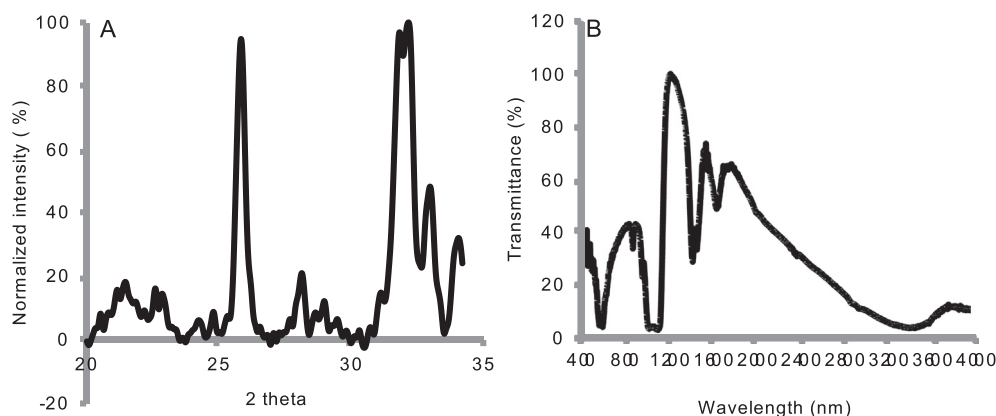


Fig. 3. HA deposition on nanotubular titania characterized by (A) XRD analysis, and by (B) FT-IR spectroscopy.

### 3.4. Broth microdilution antibacterial assay for antimicrobial activity of dual-functional peptides

Next, the inhibition effect of the peptides versus their varying concentration was determined according to Broth Microdilution Antibacterial Assay. In this assay,  $10^6$  cfu/mL cells were incubated with peptides at various concentrations from 1  $\mu$ g/mL to 256  $\mu$ g/mL at 37 °C for 16 to 20 h. As shown in Fig. 4a and b, AMP (HHC36/tet127) had great activity against *E. coli* and *S. mutans* as reported in literature [8,14,54,55]. However, the trend of the antimicrobial activity is observed to be different in two bacterial conditions. The best working conditions of AMP is 32  $\mu$ g/mL for *E. coli* (Fig. 4a), and 16  $\mu$ g/mL for *S. mutans* (Fig. 4b). In the case of the dual functional peptide, cHABP1-AMP, it demonstrated an antimicrobial activity in solution but the antimicrobial activity is low compared to the positive control (AMP) against *E. coli* (Fig. 4a) and *S. mutans* (Fig. 4b) in solution, as expected. The minimum inhibitory peptide concentration for cHABP1-AMP against *E. coli* is 32  $\mu$ g/mL (Fig. 4a), which is the same condition for AMP against to *E. coli*. In case of *S. mutans*, determination of the minimum inhibitory peptide concentration is difficult compare to that of *E. coli*. The sharp decrease in cHABP1-AMP absorbance as observed in the *E. coli* (Fig. 4a) was not observed with the increasing peptide concentration from 32  $\mu$ g/mL to 256  $\mu$ g/mL against *S. mutans* (Fig. 4b). A complete bacteria inhibition was not observed at the highest cHABP1-AMP peptide concentration of 256  $\mu$ g/mL (Fig. 4b). But, it is clear that the engineered peptide with dual functionality had a remarkable antibacterial activity in solution especially in the presence of *E. coli* (Fig. 4a). In addition, we have surprisingly observed cHABP1 partially inhibited bacterial reproduction as a negative control which was predicted through hydropathy index analyses. Compared to only cHABP1, the number of cells for the dual functional peptide at higher concentrations of peptide (128  $\mu$ g/mL and 256  $\mu$ g/mL), in each type of bacteria conditions, were magnitudes of two times lower (Fig. 4a and b).

The antimicrobial activities of dual functional peptide were analyzed over a continuous bacterial growth for 16 h at the highest concentration (256  $\mu$ g/mL) in the presence of *E. coli* and *S. mutans* (Fig. 5). Dual functional peptide (cHABP1-AMP) inhibits around 90% and 75% bacterial growth in case of *E. coli* and *S. mutans*, respectively (Fig. 5).

Table 1

Molecular characteristics of the engineered peptides (AMP, cHABP1, cHABP1-AMP).

Peptide name	Sequence	MW <sup>a</sup>	pI <sup>a</sup>	GRAVY <sup>a</sup>	Chr <sup>a</sup>
AMP	KRWKWWRR	1487.78	12.31	-2.767	+5
cHABP1	CMLPHHGAC	968.17	6.90	0.456	0
cHABP1-Spacer-AMP	CMLPHHGAC-GGG-KRWKWWRR	2609.09	10.93	-1.048	+5

<sup>a</sup> MW: molecular weight; pI: isoelectric point; Chr: Net Charge and GRAVY: Grant Average Hydropathy Index ([expasy.org](http://expasy.org)).

### 3.5. Antimicrobial efficacy of dual-function peptide on Ca-P coated titanium surface

#### 3.5.1. Bactericidal effect

To examine the striking difference in bacterial adhesion between non-functionalized and peptide functionalized Ca-P coated nanotubular titanium surface, confocal microscopy experiments were performed. cHABP1-AMP on the surface antimicrobial activity was shown with confocal microscopy against *S. mutans* and *E. coli* (Fig. 6). cHABP1-AMP functionalized surface has similar antimicrobial activity as shown in Fig. 6 against to *S. mutans* compared to *E. coli*.

#### 3.5.2. Anti-adhesive effect

Bacterial adhesion characteristic of functionalized substrates was assessed via plate spreading method at longer time period (24 h) for *E. coli* and *S. mutans* (Fig. 7). At the end of 24 h incubation period, 30% decreases in bacteria number (*S. mutans*) were approximately observed in the presence of cHABP1 and cHABP1-AMP compared to bare (non-functionalized surface). There is no significant difference among cHABP1 and cHABP1-AMP.

In case of *E. coli* at 24 h, significant difference was observed among non-functionalized surface, cHABP1, cHABP1-AMP treated surface. 20% decrease for cHABP1 treated surface and 70% decrease for cHABP1-AMP treated surface were observed. This observation is correlated with in solution experiment. Dual functional peptide is more efficient for *E. coli* with low bacterial adhesion rate.

### 3.6. Secondary structure features

Characteristic features of peptide backbone shapes that are associated with each distinct level of antimicrobial efficacy are examples of structure-function relationships. The rule induction algorithm finds these relationships by prioritizing features according to the relevance to the antimicrobial activity level [56–58]. The rules found covered at least 5–10% of the 500 structures generated for each peptide are given in Fig. 8. Each rule specifies which secondary structures are observed with a specific antimicrobial level compared to all other observed antimicrobial levels. The secondary structures investigated are bends, turns and alpha helices. A bend is a backbone feature in which the

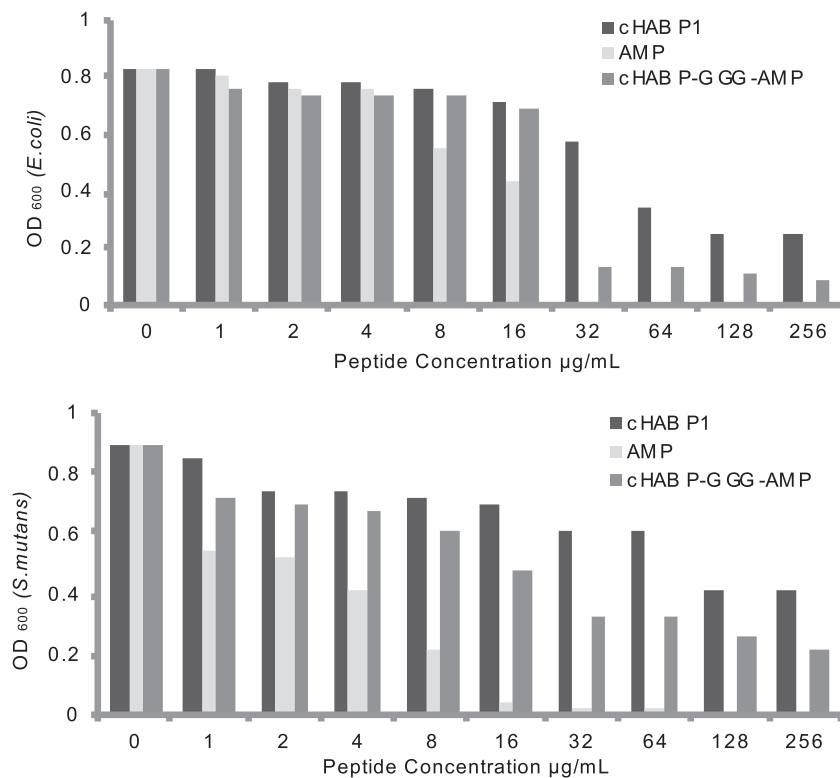


Fig. 4. Broth Microdilution Assay (A) in the presence of *E. coli* and (B) in the presence of *S. mutans* incubated with peptides at 37 °C for 16 h.

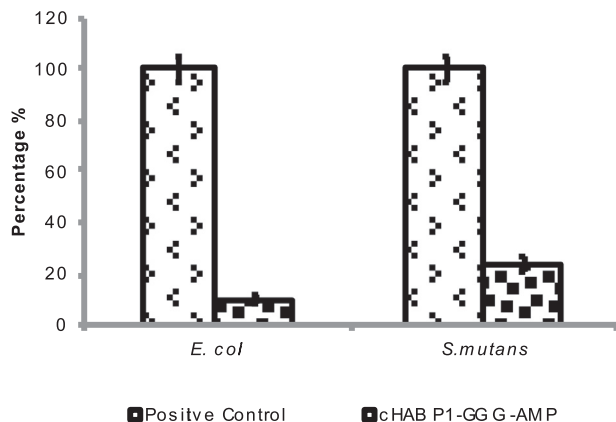


Fig. 5. The percentage of adherent *E. coli* (left) and *S. mutans* (right) after 16 h of the continuous bacterial growth in 256 µg/mL of AMP and cHABPI-AMP.

backbone curvature is high. A turn describes a bend that has hydrogen bonding between backbone atoms. An alpha helix is a turn with a regular hydrogen-bonding pattern. In Fig. 8, all of the rules were same for both of the pathogens studied because the relative order of effectiveness among all three peptides studied was kept same for them. Depending on frequencies as indicated in Fig. 8, corresponding secondary structures are provided fitting to each of the inductions rules: Rule 1 for AMP, Rule 4 and 5 for cHABPI-AMP, and Rule 6 for cHABP1.

#### 4. Discussion

We have demonstrated dual-functional peptide-based approach to functionalize Ca-P coated titanium surface to inhibit bacterial spreading and to reduce bacterial adhesion. Functionalized surface has strong bactericidal effect on gram positive (*S. mutans*) and gram-negative (*E. coli*) bacteria. The peptide application method based on self-assembly

process is simple and easy to apply for surface functionalization. Due to the method simplicity, the peptide solution can be applied to prevent implant infection immediately before the surgery. Simplicity of peptide application to implant material surface makes this peptide approach clinically feasible. Both implants and peptide solutions can be packaged and stored separately. The implant surface can be modified in the operating room before surgery and also can be used as washing solution during implantation step.

##### 4.1. Surface characteristics of nanotubular titanium and Ca-P coated Nanotubular titanium

The fabrication of TiO<sub>2</sub> nanotubular structures by the anodization method has attracted wide interest because of their high surface-to-volume ratio, controllable dimensions, adjustable wettability, and simple processing procedures [59,60]. It has been reported that TiO<sub>2</sub> nanotube arrays on titanium surfaces can significantly accelerate osteoblast cell growth and adhesion in vitro [33] and improve bone formation and bonding strength in vivo [61,62]. In addition, since titania nano-structures are formed by the anodization of the titanium substrate itself, the coating has stronger mechanical adhesion than most bio-ceramic coatings (e.g. HA coating) processed by deposition techniques such as plasma spray, electrophoretic and electrolytic deposition [49]. Due to the ceramic high adhesion probability to nanotubular titanium, we applied Ca-P coated to the nanotubular titanium surface. Ca-P coatings have been known to improve implant material biocompatibility and osteoconductivity. The presence of biologically active oxide layer and a stable crystalline base for Ca-P deposition are of critical importance in shaping the cellular interaction between the host tissue and implant, enabling transmission of forces and long term implant success [5,14,49,54,63]. On the other hand, Ca-P coatings by applying electrolytic deposition are good platform to deliver growth factors, and drugs due to the porous surface properties. This allows us to load more peptides to the implant materials by increasing surface area.

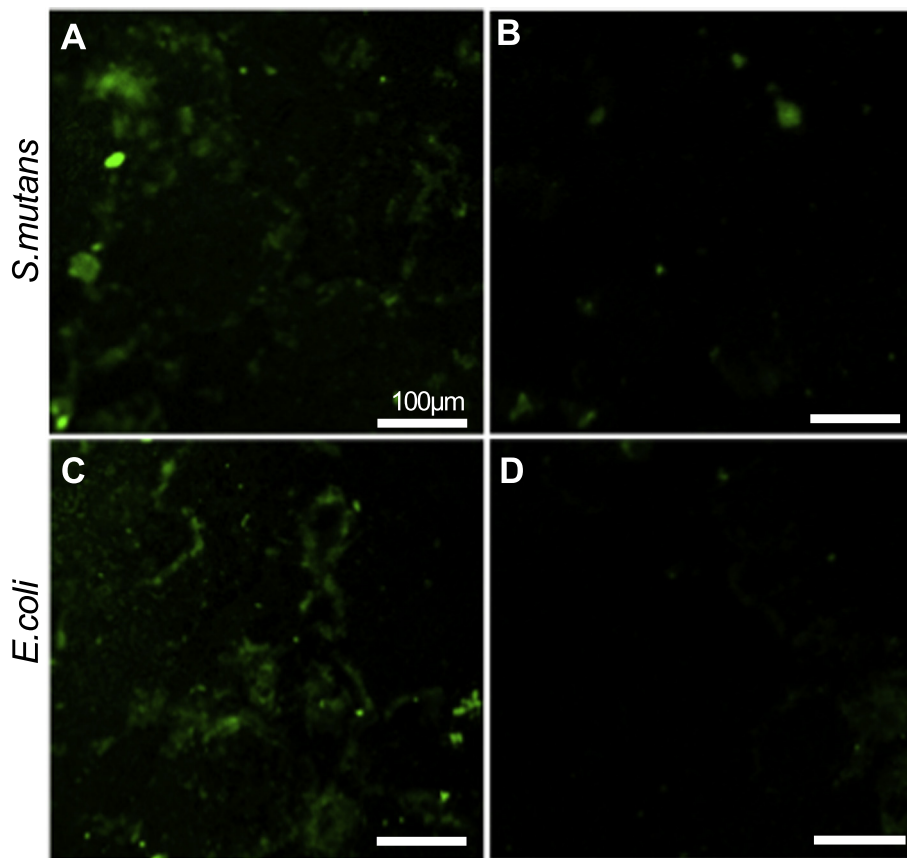


**Fig. 6.** Confocal microscopy images of Ca-P coated titanium surfaces. (A) Bare and (B) chHABP1-AMP functionalized after 2 h incubation with *S. mutans*. (C) Bare and (D) chHABP1-AMP functionalized after 2 h incubation with *E. coli*.

#### 4.2. Designing of chHABP1-AMP dual-functional peptides to functionalize the Ca-P coated nanotubular titanium surface

We have demonstrated material binding peptide-based immobilization methodology, which can be new approach for local delivery of antimicrobial agents at the implant site to prevent bacterial infection. The concerns regarding the local delivery of antibiotics in implantation are the relative inhibition of osteointegration and bacterial resistance to them. High doses of antibiotics often affect the cell viability and osteogenic activity. AMPs are promising candidates due to their potential bactericidal capability and low risk of developing antibiotic resistant pathogens. The AMP peptide (tet127/HHC36), which is chosen in this work, has been investigated for its antimicrobial

performance and its effect in vivo bone growth on calcium phosphate coated implants [14,54,55].

Extensive effort has been made to identify the antimicrobial mechanism of AMPs and surface associated AMPs [6,16,17]. It has been previously showed that AMPs has great affinity negatively charged membranes of bacteria. They act through either permeabilization of bacteria membrane or translocate across the bacterial membrane to attack cytoplasmic targets [14,47]. Electrostatic interaction in between negatively charged outer layer of the bacterium and the positively charged AMP is the initial step for activity of AMPs. High local concentration of cationic peptides attached the bacterial membrane; dramatic change in bacterial surface electrostatics will be induced [14,64]. The ability of AMPs to selectively interact with bacterial cells rather

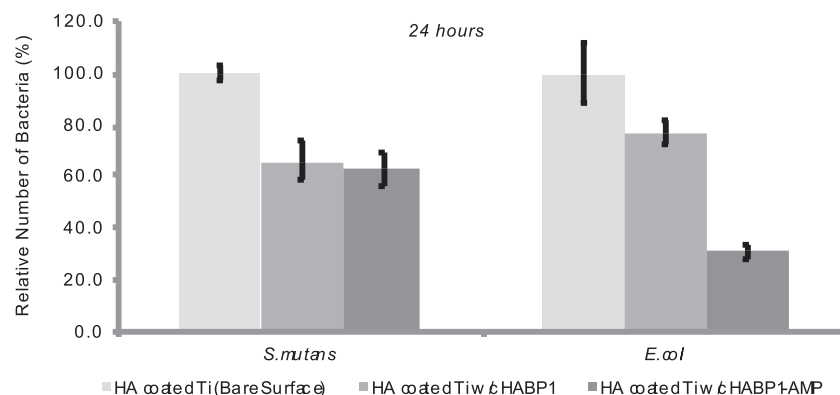


**Fig. 7.** Relative percentage of adherent bacteria on bare and functionalized surfaces (with chHABP1 and chHABP1-GGG-AMP) at 24 h in the presence of (A) *E. coli*, and (B) *S. mutans*.



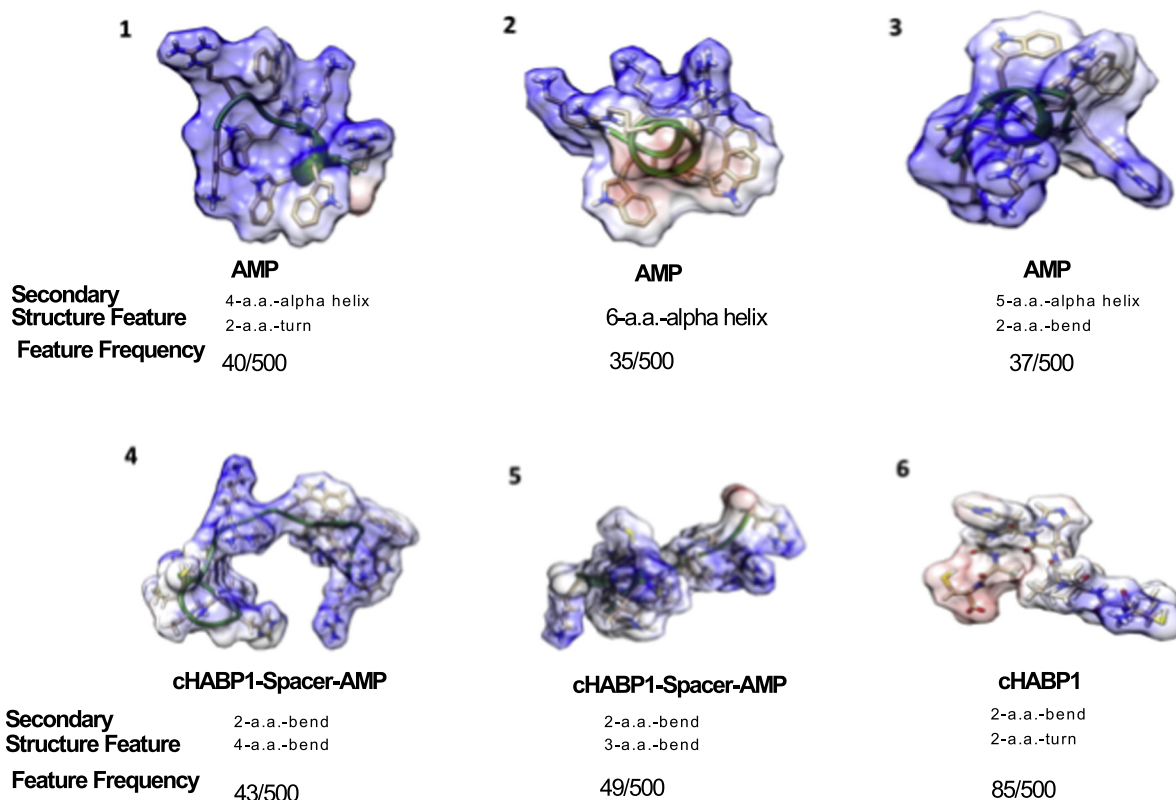


**Fig. 8.** Characteristic secondary structures fitting each of the induction rules for AMP, cHABP1-AMP, cHABP1 sequences. Induction rules for secondary structure features of AMP, cHABP1-AMP, cHABP1.

than the mammalian cells makes them preferable antimicrobial material. The major factor that contributes to selectivity property of AMPs is cationic property. The surface of bacterial membranes is more negatively charged than mammalian cells. This will lead to higher affinity of AMPs for bacterial surfaces [54,65]. Moreover, mammalian cell membranes contains high amount of cholesterol, which absent in bacteria cells, as membrane stabilizing agents and inhibitor of AMP activities. Nevertheless each type of AMPs has different cytotoxicity behavior against bacteria and mammalian cells.

In designing dual functional peptide, GGG was chosen as a flexible linker to combine cHABP1 and AMP in one molecule, where one side contains peptide (cHABP1) domain with cyclic structure. This restricts the some of conformational movement in the dual-functional peptide. Therefore, the flexible linker may allow us separate two functional domains and gain more flexible movement ability to each domain.

As we discussed above, cationic properties of peptide enhance its antimicrobial activity. In this study designed dual-functional peptide and AMP has the same cationic charge. Thus the difference in their antimicrobial activity is not only related cationic properties of peptide but also various features as conformational properties which is difficult to determine then both on the surface and while interacting with the bacteria.

The cHABP1, which is pI is 6.90, has negative charge at pH 7.4. AMP and cHABP1-AMP has cationic charge and theoretical isoelectric point of 12.31 and 10.93 respectively. Such high isoelectric point makes two peptides highly positive at working pH (7.4) and provides numerous opportunities for positively charged Arg and Lys residues to interact with the bacteria membrane. Some of the studies also refer that cationic properties of AMP help interact with the negatively charged Ca-P surfaces because of negatively charged phosphate group. The referred interaction mainly based on electrostatic interaction [14,54]. The interaction between peptide and material surfaces rely on not only electrostatic interactions between peptide and surface but also various

parameters such as peptide conformation, peptide sequence, amino acid type, charge and its location in peptide. Thus peptide-surface interactions related completed and interrelated parameters, which is expected to be different for each type of materials [39,44].

#### 4.3. Antimicrobial activity of dual-functional peptides in solution

In summary, all in solution activity cases; AMP is the most efficient antimicrobial activity at constant concentration compare with dual-functional counterpart and cHABP1. Dual-functional peptide (cHABP1-AMP) has antimicrobial activity at certain concentrations against to *S. mutans* and *E. coli*. The results reveal that AMP is more efficient for *S. mutans* as a gram-positive bacterium compare to *E. coli*. Lowest peptide concentration is 16  $\mu$ M and 32  $\mu$ M to inhibit the growth of *S. mutans* and *E. coli* respectively. The same trend was observed for each bacteria type in the presence of dual-functional peptide.

These results of AMP and its dual-functional molecular construct in solution may be compared with the information in the literature regarding the models on the AMP activity based on membrane properties of the gram-positive and the gram-negative bacteria. In general, the bacterial membranes are rich in the acidic phospholipids. Especially, the outer surface of Gram negative bacteria are composed of negatively charged lipopolysaccharides (LPS), which are held together by magnesium and calcium ions that bridge negatively charged phosphosugars. Addition of positively charged antimicrobial peptides results in displacement of divalent cations ( $Mg^{+2}$ ,  $Ca^{+2}$ ) that leads local distribution of outer membrane and promotes cell death [66,67]. Rely on the results in the literature; gram negative bacteria have faster permeabilization and killing kinetics respect to gram positive bacteria and this also confirm the conclusion of previous studies that double membrane of this gram negative bacterium is a less efficient barrier than the single membrane and thick peptidoglycan layer of the gram-positive species [67–69].



Aside from bacterial membrane properties, AMP activity is not only controlled by membrane structure of the bacteria but also through gene regulation mechanism. This has been proposed to regulate selected resistance genes, e.g. *dlt*-operon, *mprF* and *vraFG* genes, when the bacteria come into contact with the AMPs. These specific genes mostly decrease the net negative charge of the envelope and limit the interaction of AMP with the envelope [66,68,69]. Although AMPs in solution activity is dependent on various parameters in solution, correlation of in solution parameters with on the surface ones is not understood yet.

#### 4.4. Antimicrobial activity of dual-functional peptide on the surface

The surface activity of dual functional peptides was evaluated at longer time periods (24 h) in the presence of *E. coli* (gram-negative) and *S. mutans* (gram positive) (Fig. 7). In solution antimicrobial activity indicated that AMP and the dual-functional peptides were efficient for *E. coli* at  $2 \times$  lower concentration compare to *S. mutans*. In solution and on the surface activity of AMP and dual functional peptides were different. For example AMP and dual functional peptide has high antimicrobial activity against to *E. coli* compare to *S. mutans*. These results reveal that antimicrobial properties of peptide on the surface do not only depend on peptide charge. There are different parameters in addition to peptide charge involved in antimicrobial activity. Conformation of peptide on the surface and available side chain of amino acids that can interact with the bacteria membrane can be critical parameters.

On the other hand, cHABP1 has also antimicrobial activity. The charge of the peptide at pH 7.4 is negative. This finding demonstrates that the antimicrobial activity cannot be related only charge of the peptide one more time. Other parameter such as conformation of peptide has a role in determining antimicrobial properties. Our peptide structure evaluations also emphasize the importance of the peptide structure to exhibit both mineral binding and antimicrobial property.

The results indicated that antimicrobial activity of dual functional peptides is more pronounced in case of gram-positive bacteria (*S. mutans*) when they are applied on the surface.

#### 4.5. Structural features of peptides

In addition to the role of membrane structure properties and possible sensing mechanism of the bacteria in antimicrobial activity of AMPs, molecular structure of the peptides is also critical parameter that needs to be evaluated. Especially, designing new peptides with predictable ability for a specific material function is a current challenge in bioenabled material systems. Explicit structure-function relationships are resulting in substantial progress toward this challenge because the effectiveness of candidate peptides is not obvious without experimental determination of the function level. Methods for evaluating candidate peptides before experimental determination make this challenge more tractable because the number of candidate peptides increase exponentially for every undetermined amino acid in a chimeric peptide. For maximum uncertainty about twelve amino acid positions, the number of candidates to be determined is  $> 10^{15}$ . The antimicrobial activity function relationships provide features to evaluate candidate peptides against before synthesizing them. According to the observation shown in Fig. 8, AMP fits to three of the rules having alpha helix feature, which was not observed in the cHABP1-AMP peptide or cHABP1 peptide structures [70]. These results explain us the role of peptide structure as one parameter for the low antimicrobial efficacy of dual functional peptides. The antimicrobial features of dual functional peptides are strongly correlated with its structure. Therefore, structural features of dual functional peptides can be enhanced with new spacer designs to improve antimicrobial activity.

## 5. Conclusion

Calcium phosphate coatings are widely accepted for improved osteoconductivity at the metallic implant interfaces, which may be accompanied with nanoscaled textures for improved osteointegration. Nevertheless, these surface modifications make even harder to deliver biological functional agents including antimicrobial peptides effectively at the implantation site. Here, we engineered a dual functional peptide that utilizes the biomolecular self-assembly for local therapy to prevent bacterial infection at the implant material interface coated with a common bioceramic. To achieve this, calcium phosphate coating was successfully formed on nanotubular titanium by electrolytic deposition. The engineered peptide was self-assembled on the Ca-P coating in a single step process. Consequently, implant surface was found to significantly reduce the bacterial adhesion in the presence of gram-positive and gram-negative bacteria. In addition to our experimental analysis, our peptide structure function analyses also demonstrated that antimicrobial features of the engineered peptides are strongly correlated with their structures. Interestingly, AMP fits to three of the rules having alpha helix feature, which was not observed in the cHABP1-AMP peptide or cHABP1 peptide structures [70]. These results explain us the role of peptide structure as one parameter for the differences in antimicrobial efficacy of dual functional peptides. The structure-function relationships may contribute to rational design of dual functional peptide with optimized biofunctionality. Due to the simplicity of the method, bio-enabled approach can be used as self-assembled antimicrobial solution both prior and during the orthopedic surgery. The approach could be coupled with existing therapies and holds a promise by offering an alternative to fight against bacterial resistance and infection.

## Acknowledgement

This research was supported by National Institutes of Health (NIH)–National Institute of Arthritis and Musculoskeletal and Skin Diseases AR062249 and NIH–National Institute of Dental and Craniofacial Research R01DE025476 through University of Kansas, TUBITAK BİDEP 2218 Postdoctoral Research Project and ITU Institute for Graduate Programs.

## Appendix A. Supplementary data

Further information is provided in the Supporting Information Section including MALDI-TOF analyses of synthesized peptides and histograms of Alpha Helix Frequency for each peptide. This material is available free of charge via the Internet at <http://pubs.acs.org>. Supplementary data to this article can be found online at <https://doi.org/10.1016/j.msec.2018.09.030>.

## References

- [1] M. Geetha, A.K. Singh, R. Asokamani, A.K. Gogia, Ti based biomaterials, the ultimate choice for orthopaedic implants - a review, *Prog. Mater. Sci.* 54 (3) (2009) 397–425, <https://doi.org/10.1016/j.pmatsci.2008.06.004>.
- [2] T. Webster, H. Yazici, *Biomedical Nanomaterials From Design to Implementation*, IET (The Institution of Engineering and Technology), London, UK, 2016.
- [3] E.M. Hetrick, M.H. Schoenfish, Reducing implant-related infections: active release strategies, *Chem. Soc. Rev.* 35 (9) (2006) 780–789, <https://doi.org/10.1039/b515219b>.
- [4] D. Campoccia, L. Montanaro, C.R. Arciola, The significance of infection related to orthopedic devices and issues of antibiotic resistance, *Biomaterials* 27 (11) (2006) 2331–2339, <https://doi.org/10.1016/j.biomaterials.2005.11.044>.
- [5] R.A. Surmenev, M.A. Surmeneva, A.A. Ivanova, Significance of calcium phosphate coatings for the enhancement of new bone osteogenesis - a review, *Acta Biomater.* 10 (2) (2014) 557–579, <https://doi.org/10.1016/j.actbio.2013.10.036>.
- [6] S.A. Onaizi, S.S.J. Leong, Tethering antimicrobial peptides: current status and potential challenges, *Biotechnol. Adv.* 29 (1) (2011) 67–74, <https://doi.org/10.1016/j.biotechadv.2010.08.012>.
- [7] H. Yazici, E. Alpaslan, G. Bhardwaj, T.J. Webster, Conventional and nano-based approaches to prevent bacterial infection, in: T. Webster, H. Yazici (Eds.),

- Biomedical Nanomaterials: From Design to Implementation, IET (The Institution of Engineering and Technology), London, UK, 2016, pp. 195–213.
- [8] M. Ma, M. Kazemzadeh-Narbat, Y. Hui, S. Lu, C. Ding, D.D.Y. Chen, R.E.W. Hancock, R. Wang, Local delivery of antimicrobial peptides using self-organized TiO<sub>2</sub> nanotube arrays for peri-implant infections, *J. Biomed. Mater. Res. A* 100A (2) (2012) 278–285, <https://doi.org/10.1002/jbm.a.33251>.
  - [9] R.E.W. Hancock, H.G. Sahl, Antimicrobial and host-defense peptides as new anti-infective therapeutic strategies, *Nat. Biotechnol.* 24 (12) (2006) 1551–1557, <https://doi.org/10.1038/nbt1267>.
  - [10] E.F. Haney, R.E.W. Hancock, Peptide design for antimicrobial and immunomodulatory applications, *Biopolymers* 100 (6) (2013) 572–583, <https://doi.org/10.1002/bip.22250>.
  - [11] H. Yazici, M.B. O'Neill, T. Kacar, B.R. Wilson, E.E. Oren, M. Sarikaya, C. Tamerler, Engineered chimeric peptides as antimicrobial surface coating agents toward infection-free implants, *ACS Appl. Mater. Interfaces* 8 (8) (2016) 5070–5081, <https://doi.org/10.1021/acsami.5b03697>.
  - [12] Z.H. Liu, S.Q. Ma, S. Duan, X.L. Deng, Y.C. Sun, X. Zhang, X.H. Xu, B.B. Guan, C. Wang, M.L. Hu, X.Y. Qi, X. Zhang, P. Gao, Modification of titanium substrates with chimeric peptides comprising antimicrobial and titanium-binding motifs connected by linkers to inhibit biofilm formation, *ACS Appl. Mater. Interfaces* 8 (8) (2016) 5124–5136, <https://doi.org/10.1021/acsami.5b11949>.
  - [13] D. Campoccia, L. Montanaro, P. Speziale, C.R. Arciola, Antibiotic-loaded biomaterials and the risks for the spread of antibiotic resistance following their prophylactic and therapeutic clinical use, *Biomaterials* 31 (25) (2010) 6363–6377, <https://doi.org/10.1016/j.biomaterials.2010.05.005>.
  - [14] M. Kazemzadeh-Narbat, J. Kindrachuk, K. Duan, H. Jenssen, R.E.W. Hancock, R. Wang, Antimicrobial peptides on calcium phosphate-coated titanium for the prevention of implant-associated infections, *Biomaterials* 31 (36) (2010) 9519–9526, <https://doi.org/10.1016/j.biomaterials.2010.08.035>.
  - [15] S.L. Haynie, G.A. Crum, B.A. Dole, Antimicrobial activities of amphiphilic peptides covalently bonded to a water-insoluble resin, *Antimicrob. Agents Chemother.* 39 (2) (1995) 301–307.
  - [16] F. Costa, I.F. Carvalho, R.C. Montelaro, P. Gomes, M.C.L. Martins, Covalent immobilization of antimicrobial peptides (AMPs) onto biomaterial surfaces, *Acta Biomater.* 7 (4) (2011) 1431–1440, <https://doi.org/10.1016/j.actbio.2010.11.005>.
  - [17] A. Shukla, K.E. Fleming, H.F. Chuang, T.M. Chau, C.R. Loose, G.N. Stephanopoulos, P.T. Hammond, Controlling the release of peptide antimicrobial agents from surfaces, *Biomaterials* 31 (8) (2010) 2348–2357, <https://doi.org/10.1016/j.biomaterials.2009.11.082>.
  - [18] K.V. Holmberg, M. Abdolhosseini, Y. Li, X. Chen, S.-U. Gorr, C. Aparicio, Bio-inspired stable antimicrobial peptide coatings for dental applications, *Acta Biomater.* 9 (9) (2013) 8224–8231, <https://doi.org/10.1016/j.actbio.2013.06.017>.
  - [19] M. Godoy-Gallardo, C. Mas-Moruno, M.C. Fernandez-Calderon, C. Perez-Giraldo, J.M. Manero, F. Albericio, F.J. Gil, D. Rodriguez, Covalent immobilization of hLf1-11 peptide on a titanium surface reduces bacterial adhesion and biofilm formation, *Acta Biomater.* 10 (8) (2014) 3522–3534, <https://doi.org/10.1016/j.actbio.2014.03.026>.
  - [20] K. Lim, R.R.Y. Chua, B. Ho, P.A. Tambyah, K. Hadinoto, S.S.J. Leong, Development of a catheter functionalized by a polydopamine peptide coating with antimicrobial and antibiofilm properties, *Acta Biomater.* 15 (2015) 127–138, <https://doi.org/10.1016/j.actbio.2014.12.015>.
  - [21] L. Wang, J. Chen, C. Cai, L. Shi, S. Liu, L. Ren, Y. Wang, Multi-biofunctionalization of a titanium surface with a mixture of peptides to achieve excellent antimicrobial activity and biocompatibility, *J. Mater. Chem. B* 3 (1) (2015) 30–33, <https://doi.org/10.1039/c4tb01318b>.
  - [22] B.E. Nie, H.Y. Ao, C. Chen, K. Xie, J.L. Zhou, T. Long, T.T. Tang, B. Yue, Covalent immobilization of KR-12 peptide onto a titanium surface for decreasing infection and promoting osteogenic differentiation, *RSC Adv.* 6 (52) (2016) 46733–46743, <https://doi.org/10.1039/c6ra06778f>.
  - [23] M. Mateescu, S. Baixe, T. Garnier, L. Jierry, V. Ball, Y. Haikel, M.H. Metz-Boutigue, M. Nardin, P. Schaaf, O. Etienne, P. Laval, Antibacterial peptide-based gel for prevention of medical implanted-device infection, *PLoS One* 10 (12) (2015) 1–13, <https://doi.org/10.1371/journal.pone.0145143>.
  - [24] A.K. Muszanska, E.T.J. Rochford, A. Gruszka, A.A. Bastian, H.J. Busscher, W. Norde, H.C. van der Mei, A. Herrmann, Antiadhesive polymer brush coating functionalized with antimicrobial and RGD peptides to reduce biofilm formation and enhance tissue integration, *Biomacromolecules* 15 (6) (2014) 2019–2026, <https://doi.org/10.1021/bm500168s>.
  - [25] L. Zhang, C.Y. Ning, T. Zhou, X.M. Liu, K.W.K. Yeung, T.J. Zhang, Z.S. Xu, X.B. Wang, S.L. Wu, P.K. Chu, Polymeric nanoarchitectures on Ti-based implants for antibacterial applications, *ACS Appl. Mater. Interfaces* 6 (20) (2014) 17323–17345, <https://doi.org/10.1021/am5045604>.
  - [26] D. Alves, M.O. Pereira, Mini-review: antimicrobial peptides and enzymes as promising candidates to functionalize biomaterial surfaces, *Biofouling* 30 (4) (2014) 483–499, <https://doi.org/10.1080/08927014.2014.889120>.
  - [27] J.C. Love, L.A. Estroff, J.K. Kriebel, R.G. Nuzzo, G.M. Whitesides, Self-assembled monolayers of thiols on metals as a form of nanotechnology, *Chem. Rev.* 105 (4) (2005) 1103–1169, <https://doi.org/10.1021/cr0300789>.
  - [28] L. Zhao, P.K. Chu, Y. Zhang, Z. Wu, Antibacterial coatings on titanium implants, *J. Biomed. Mater. Res. B Appl. Biomater.* 91 (1) (2009) 470–480.
  - [29] M. Stigter, J. Bezemer, K. de Groot, P. Layrolle, Incorporation of different antibiotics into carbonated hydroxyapatite coatings on titanium implants, release and antibiotic efficacy, *J. Control. Release* 99 (1) (2004) 127–137, <https://doi.org/10.1016/j.jconrel.2004.06.011>.
  - [30] H. Liu, H. Yazici, C. Ergun, T.J. Webster, H. Bermek, An in vitro evaluation of the Ca/P ratio for the cytocompatibility of nano-to-micron particulate calcium phosphates for bone regeneration, *Acta Biomater.* 4 (5) (2008) 1472–1479, <https://doi.org/10.1016/j.actbio.2008.02.025>.
  - [31] G. Bhardwaj, H. Yazici, T.J. Webster, Reducing bacteria and macrophage density on nanophase hydroxyapatite coated onto titanium surfaces without releasing pharmaceutical agents, *Nanoscale* 7 (18) (2015) 8416–8427, <https://doi.org/10.1039/c5nr00471c>.
  - [32] S.B. Goodman, Z. Yao, M. Keeney, F. Yang, The future of biologic coatings for orthopaedic implants, *Biomaterials* 34 (13) (2013) 3174–3183, <https://doi.org/10.1016/j.biomaterials.2013.01.074>.
  - [33] J. Raphael, M. Holodniy, S.B. Goodman, S.C. Heilshorn, Multifunctional coatings to simultaneously promote osseointegration and prevent infection of orthopaedic implants, *Biomaterials* 84 (2016) 301–314, <https://doi.org/10.1016/j.biomaterials.2016.01.016>.
  - [34] Y. Zhou, M.L. Snead, C. Tamerler, Bio-inspired hard-to-soft interface for implant integration to bone, *Nanomedicine* 11 (2) (2015) 431–434, <https://doi.org/10.1016/j.nano.2014.10.003>.
  - [35] C. Wisdom, S.K. VanOosten, K.W. Boone, D. Khvostenko, P.M. Arnold, M.L. Snead, C. Tamerler, Controlling the biomimetic implant interface: modulating antimicrobial activity by spacer design, *J. Mol. Eng. Mater.* 4 (1) (2016), <https://doi.org/10.1142/s2251237316400050>.
  - [36] M. Sarikaya, C. Tamerler, A.K.Y. Jen, K. Schulten, F. Baneyx, Molecular biomimetics: nanotechnology through biology, *Nat. Mater.* 2 (9) (2003) 577–585, <https://doi.org/10.1038/nmat964>.
  - [37] S. Donatan, H. Yazici, H. Bermek, M. Sarikaya, C. Tamerler, M. Urgan, Physical elution in phase display selection of inorganic-binding peptides, *Mater. Sci. Eng. C* 29 (1) (2009) 14–19, <https://doi.org/10.1016/j.msec.2008.05.003>.
  - [38] K. Shiba, Exploitation of peptide motif sequences and their use in nanobiotechnology, *Curr. Opin. Biotechnol.* 21 (4) (2010) 412–425, <https://doi.org/10.1016/j.copbio.2010.07.008>.
  - [39] D. Khatayevich, M. Gungormus, H. Yazici, C. So, S. Cetinel, H. Ma, A. Jen, C. Tamerler, M. Sarikaya, Biofunctionalization of materials for implants using engineered peptides, *Acta Biomater.* 6 (12) (2010) 4634–4641, <https://doi.org/10.1016/j.actbio.2010.06.004>.
  - [40] C. Tamerler, D. Khatayevich, M. Gungormus, T. Kacar, E.E. Oren, M. Hnilova, M. Sarikaya, Molecular biomimetics: GEPI-based molecular routes to technology, *Biopolymers* 94 (1) (2010) 78–94, <https://doi.org/10.1002/bip.21368>.
  - [41] M. Gungormus, H. Fong, I.W. Kim, J.S. Evans, C. Tamerler, M. Sarikaya, Regulation of in vitro calcium phosphate mineralization by combinatorially selected hydroxyapatite-binding peptides, *Biomacromolecules* 9 (3) (2008) 966–973, <https://doi.org/10.1021/bm701037x>.
  - [42] M. Gungormus, E.E. Oren, J.A. Horst, H. Fong, M. Hnilova, M.J. Somerman, M.L. Snead, R. Samudrala, C. Tamerler, M. Sarikaya, Cementomimetics-constructing a cementum-like biomineralized microlayer via amelogenin-derived peptides, *Int. J. Oral Sci.* 4 (2) (2012) 69–77, <https://doi.org/10.1038/ijos.2012.40>.
  - [43] F.S. Utku, E. Yuca, E. Seckin, G. Goller, A.Y. Karatas, M. Urgan, C. Tamerler, Protein-mediated hydroxyapatite composite layer formation on nanotubular titania, *Bioinspir. Biomim.* Nan. 4 (2) (2015) 155–165, <https://doi.org/10.1680/bbn.15.00001>.
  - [44] H. Yazici, H. Fong, B. Wilson, E.E. Oren, F.A. Amos, H. Zhang, J.S. Evans, M.L. Snead, M. Sarikaya, C. Tamerler, Biological response on a titanium implant-grade surface functionalized with modular peptides, *Acta Biomater.* 9 (2) (2013) 5341–5352, <https://doi.org/10.1016/j.actbio.2012.11.004>.
  - [45] M. Gungormus, M. Branco, H. Fong, J.P. Schneider, C. Tamerler, M. Sarikaya, Self assembled bi-functional peptide hydrogels with biomineralization-directing peptides, *Biomaterials* 31 (28) (2010) 7266–7274, <https://doi.org/10.1016/j.biomaterials.2010.06.010>.
  - [46] H. Geng, Y. Yang, Aidin Aday, Xu Zhang, Xin Song, Lei Gong, Zhang Xi, Ping Gao, Engineered chimeric peptides with antimicrobial and titanium-binding functions to inhibit biofilm formation on Ti implants, *Mater. Sci. Eng. C* 82 (2018) 141–154, <https://doi.org/10.1016/j.msec.2017.08.062>.
  - [47] E. Yuca, A. Y. Karatas, U.O. Seker, M. Gungormus, G. Dinler-Doganay, M. Sarikaya, C. Tamerler, In vitro labeling of hydroxyapatite minerals by an engineered protein, *Biotechnol. Bioeng.*, 108 (5): 1021–1030. > <https://doi.org/10.1002/bit.23041>.
  - [48] A. Cherkasov, K. Hilpert, H. Jenssen, C.D. Fjell, M. Waldbrook, S.C. Mullaly, R. Volkmer, R.E.W. Hancock, Use of artificial intelligence in the design of small peptide antibiotics effective against a broad spectrum of highly antibiotic-resistant superbugs, *ACS Chem. Biol.* 4 (1) (2009) 65–74, <https://doi.org/10.1021/cb800240j>.
  - [49] F.S. Utku, E. Seckin, G. Goller, C. Tamerler, M. Urgan, Carbonated hydroxyapatite deposition at physiological temperature on ordered titanium oxide nanotubes using pulsed electrochemistry, *Ceram. Int.* 40 (10) (2014) 15479–15487, <https://doi.org/10.1016/j.ceramint.2014.07.004>.
  - [50] W. Kabsch, C. Sander, Dictionary of protein secondary structure: pattern recognition of hydrogen-bonded and geometrical features, *Biopolymers* 22 (12) (1983) 2577–2637.
  - [51] J.W. Grzymala-Busse, W. Rzasa, A local version of the MLEM 2 algorithm for rule induction, *Fund. Inform.* 100 (1–4) (2010) 99–116.
  - [52] R. Hahn, T. Stergiououlis, J.M. Macak, D. Tsoukleris, A.G. Kontos, S.P. Albu, D. Kim, A. Ghicov, J. Kunze, P. Falaras, P. Schumki, Efficient solar energy conversion using TiO<sub>2</sub> nanotubes produced by rapid breakdown anodization - a comparison, *Phys. Status Solidi Rapid Res. Lett.* 1 (4) (2007) 135–137, <https://doi.org/10.1002/psrr.200701074>.
  - [53] F.S. Utku, E. Seckin, G. Goller, C. Tamerler, M. Urgan, Electrochemically designed interfaces: hydroxyapatite coated macro-mesoporous titania surfaces, *Appl. Surf. Sci.* 350 (2015) 62–68, <https://doi.org/10.1016/j.apsusc.2015.04.131>.
  - [54] M. Kazemzadeh-Narbat, S. Noordin, B.A. Masri, D.S. Garbuz, C.P. Duncan,

- R.E.W. Hancock, R. Wang, Drug release and bone growth studies of antimicrobial peptide-loaded calcium phosphate coating on titanium, *J. Biomed. Mater. Res. B Appl. Biomater.* 100B (5) (2012) 1344–1352, <https://doi.org/10.1002/jbm.b.32701>.
- [55] M. Kazemzadeh-Narbat, B.F.L. Lai, C. Ding, J.N. Kizhakkedathu, R.E.W. Hancock, R. Wang, Multilayered coating on titanium for controlled release of antimicrobial peptides for the prevention of implant-associated infections, *Biomaterials* 34 (24) (2013) 5969–5977, <https://doi.org/10.1016/j.biomaterials.2013.04.036>.
- [56] M. Nategholeslam, *A Non-equilibrium Work Study of Antimicrobial Peptide-Membrane Interactions*, University of Guelph, 2014.
- [57] M. Nichols, M. Kuljanin, M. Nategholeslam, T. Hoang, S. Vafaei, B. Tomberli, C.G. Gray, L. DeBruin, M. Jelokhani-Niaraki, Dynamic turn conformation of a short tryptophan-rich cationic antimicrobial peptide and its interaction with phospholipid membranes, *J. Phys. Chem. B* 117 (47) (2013) 14697–14708, <https://doi.org/10.1021/jp4096985>.
- [58] K. Hilpert, M. Elliott, H. Jenssen, J. Kindrachuk, C.D. Fjell, J. Korner, D.F.H. Winkler, L.L. Weaver, P. Henklein, A.S. Ulrich, S.H.Y. Chiang, S.W. Farmer, N. Pante, R. Volkmer, R.E.W. Hancock, Screening and characterization of surface-tethered cationic peptides for antimicrobial activity, *Chem. Biol.* 16 (1) (2009) 58–69, <https://doi.org/10.1016/j.chembiol.2008.11.006>.
- [59] J.M. Macak, H. Tsuchiya, A. Ghicov, K. Yasuda, R. Hahn, S. Bauer, P. Schmuki, TiO<sub>2</sub> nanotubes: self-organized electrochemical formation, properties and applications, *Curr. Opin. Solid State Mater. Sci.* 11 (1–2) (2007) 3–18, <https://doi.org/10.1016/j.cossms.2007.08.004>.
- [60] S.E. Kim, J.H. Lim, S.C. Lee, S.-C. Nam, H.-G. Kang, J. Choi, Anodically nanostructured titanium oxides for implant applications, *Electrochim. Acta* 53 (14) (2008) 4846–4851, <https://doi.org/10.1016/j.electacta.2008.02.005>.
- [61] L.M. Bjursten, L. Rasmusson, S. Oh, G.C. Smith, K.S. Brammer, S. Jin, Titanium dioxide nanotubes enhance bone bonding in vivo, *J. Biomed. Mater. Res. A* 92A (3) (2010) 1218–1224, <https://doi.org/10.1002/jbm.a.32463>.
- [62] K.S. Brammer, S. Oh, C.J. Cobb, L.M. Bjursten, H. van der Heyde, S. Jin, Improved bone-forming functionality on diameter-controlled TiO<sub>2</sub> nanotube surface, *Acta Biomater.* 5 (8) (2009) 3215–3223, <https://doi.org/10.1016/j.actbio.2009.05.008>.
- [63] M. Yoshinari, T. Kato, K. Matsuzaka, T. Hayakawa, K. Shiba, Prevention of biofilm formation on titanium surfaces modified with conjugated molecules comprised of antimicrobial and titanium-binding peptides, *Biofouling* 26 (1) (2010) 103–110, <https://doi.org/10.1080/08927010903216572>.
- [64] J.D.F. Hale, R.E.W. Hancock, Alternative mechanisms of action of cationic antimicrobial peptides on bacteria, *Expert Rev. Anti-Infect. Ther.* 5 (6) (2007) 951–959, <https://doi.org/10.1586/14787210.5.6.951>.
- [65] E. Glukhov, M. Stark, L.L. Burrows, C.M. Deber, Basis for selectivity of cationic antimicrobial peptides for bacterial versus mammalian membranes, *J. Biol. Chem.* 280 (40) (2005) 33960–33967, <https://doi.org/10.1074/jbc.M507042200>.
- [66] M. Li, D.J. Cha, Y. Lai, A.E. Villaruz, D.E. Sturdevant, M. Otto, The antimicrobial peptide-sensing system of *Staphylococcus aureus*, *Mol. Microbiol.* 66 (5) (2007) 1136–1147, <https://doi.org/10.1111/j.1365-2958.2007.05986.x>.
- [67] J.P.S. Powers, R.E.W. Hancock, The relationship between peptide structure and antibacterial activity, *Peptides* 24 (11) (2003) 1681–1691, <https://doi.org/10.1016/j.peptides.2003.08.023>.
- [68] M. Li, Y.P. Lai, A.E. Villaruz, D.J. Cha, D.E. Sturdevant, M. Otto, Gram-positive three-component antimicrobial peptide-sensing system, *Proc. Natl. Acad. Sci. U. S. A.* 104 (22) (2007) 9469–9474, <https://doi.org/10.1073/pnas.0702159104>.
- [69] M. Zasloff, Antimicrobial peptides of multicellular organisms, *Nature* 415 (6870) (2002) 389–395, <https://doi.org/10.1038/415389a>.
- [70] D.T. Yucesoy, M. Hnilova, K. Boone, P.M. Arnold, M.L. Snead, C. Tamerler, Chimeric peptides as implant functionalization agents for titanium alloy implants with antimicrobial properties, *JOM* 67 (4) (2015) 754–766, <https://doi.org/10.1007/s11837-015-1350-7>.